On the use of interconnected reinforcements to enhance the performance of monolithic aluminum

M. Gupta[1], L. Adi[1], V. V. Ganesh[2] and T. S. Srivatsan[3,*]

[1]Department of Mechanical Engineering, National University of Singapore, 10, Kent Ridge Crescent, Singapore 119260
[2]Department of Chemical and Materials Engineering, Arizona State University, Tempe, Arizona 85287, USA
[3]Department of Mechanical Engineering, The University of Akron, Akron, Ohio 443256-3903, USA

In this article, an innovative concept of using interconnected reinforcement architecture as a potentially viable reinforcement for a non heat-treatable aluminum alloy is presented and discussed. The candidate aluminum alloy chosen is 1050 and the reinforcement are wires of galvanized iron. The technique of conventional casting followed by hot extrusion was used to synthesize the composite material. The extruded aluminum alloy composite exhibited good interfacial integrity between the matrix metal and the wire-reinforcing phase. Thermo-mechanical analysis revealed a lower coefficient of thermal expansion for the aluminum alloy composite material when compared to the monolithic counterpart. Mechanical property characterization revealed enhanced matrix hardness, elastic modulus, yield strength and ultimate tensile strength of the reinforced aluminum alloy metal matrix when compared to the un-reinforced counterpart, i.e. monolithic aluminum. The conjoint influence of reinforcement architecture in the metal matrix and volume fraction on properties is rationalized in light of intrinsic microstructural effects, nature of loading and macroscopic aspects of fracture.

THE emergence of composite materials resulted from a need to have materials that offered a combination of improved mechanical properties such as specific modulus (E/ρ), strength, resistance to fatigue, improved resistance to wear and corrosion, and enhanced performance at elevated temperatures[1–3]. Sustained research and development efforts in the time period spanning the last three decades has resulted in the emergence of metal matrix composites (MMCs) as a potentially viable and economically affordable candidate for a spectrum of performance critical engineering applications. This is due to their innate ability to exhibit properties that can easily be tailored by changing the type, nature, volume fraction and architecture of the reinforcing phase with concurrent changes in microstructure of the matrix[3–8]. Candidate reinforcement choices for metal matrices are particulates, whiskers or short fibres, and continuous fibres[1–3,8–10]. In continuous fibre-reinforced metal matrices, the reinforcing phase can be aligned along specific directions to meet and/or exceed the property requirements of the end-application. Generally, the elastic modulus (E) of the fibre-reinforced metal matrix conforms well with the rule-of-mixtures (ROM) prediction, when the composite material is loaded in the direction of the reinforcing fibres[11,12]. Spurred by the interest in MMCs, recent investigations have attempted to use a unique approach of interconnecting the reinforcing fibres. The resultant modulus of the reinforced metal matrix was noticeably higher than the value predicted by the theory of rule-of-mixtures ROM. Besides, the reinforced metal matrix revealed significant improvements in coefficient of thermal expansion (CTE), tensile strength and damping capacity[13–15]. The observed improvement in these properties was realized even for low volume fractions ($\ll 5\%$) of the reinforcing phase, while retaining the primary processing technique to be that of conventional casting. Results documented in the published literature reveal that in all of these studies, the emphasis has been on examining: (a) intrinsic influence of nature of reinforcement, and (b) reinforcement architecture and interconnectivity, on both physical and mechanical properties of metal matrices, such as aluminum, magnesium and titanium[9,10]. However, there exists no systematic analysis to comprehensively examine the effect of volume fraction of interconnected reinforcement on mechanical response of the MMC material.

Accordingly, the objective of the present study was to synthesize using the technique of conventional casting and also characterize an aluminum alloy reinforced with three different volume fractions of three-dimensional reinforcement preforms composed of interconnected galvanized iron wires having a square mesh opening. The as-cast aluminum alloy composite material was then hot-extruded. The initial microstructure of the as-extruded composite and its mechanical properties were determined. Particular emphasis was placed to investigate the volume fraction of interconnected metallic wire preforms on microstructural development, physical and mechanical properties of the chosen aluminum alloy.

Experimental procedures

Material selection

In this study, high purity aluminum alloy 1050 (99.5 weight% aluminum) was chosen to be the matrix material and galva-

*For correspondence. (e-mail: tss1@uakron.edu)

nized iron wire (AISI 1008) of diameter 0.06 mm, with an equivalent of 10.80 volume percentage zinc in the form of coating, as the reinforcing phase. Three types of reinforcement patterns or architecture were chosen, having 1.6, 3.1 and 4.7 volume percentage of the wire reinforcement. A profile of the reinforcement architecture is shown in Figure 1.

Materials processing

The aluminum alloy-based metal matrix composites (AAMMCs) were synthesized using the conventional casting technique in accordance with the following sequence: (i) thoroughly cleaned pieces of the aluminum alloy 1050 were initially super-heated to 750°C in a graphite crucible; (ii) the reinforcement preform was kept inside a steel mould (40 mm in diameter), (iii) upon reaching the superheat temperature, the molten melt was continuously stirred for 2 min, using a twin-blade impeller, to facilitate homogenization of the temperature. The impeller was coated with Zirtex 25 (86% ZrO_2, 8.8% Y_2O_3, 3.6% SiO_2, 1.2% K_2Na_2O, and a trace (0.3%) of inorganic) to prevent the iron from contaminating the molten metal. Following stirring, the melt was slowly poured from the crucible into the mould. The resultant composite material was removed from the mould. Synthesis of the composite material was carried out in an atmosphere of argon gas to minimize oxidation of the aluminum alloy. Similar parameters were used for synthesizing the monolithic aluminum alloy, except that no preform was placed in the mould. The ingots obtained following the conventional casting process were precision-machined to a diameter of 35 mm and then hot-extruded at 350°C on a 150-ton hydraulic press at an extrusion ratio of 13 : 1. Colloidal graphite was used as the lubricant during hot-extrusion. The composite ingots were heated at 400°C for 45 min in a constant temperature furnace prior to extrusion.

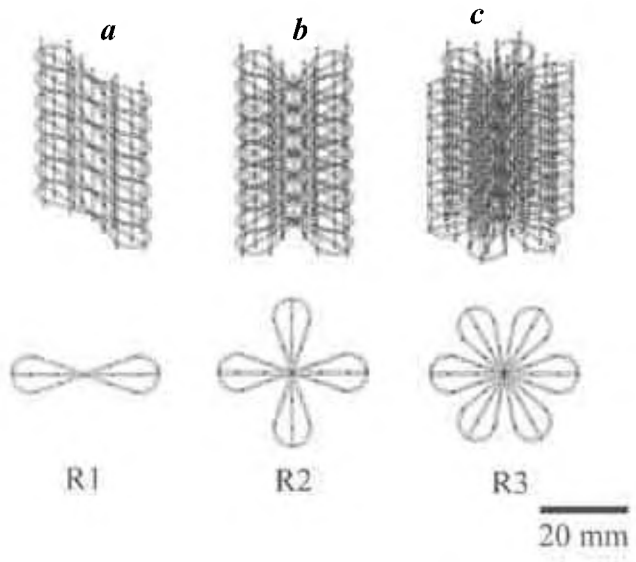

Figure 1. Schematic diagram showing types of reinforcement structures: (***a***) Al/1.6% Fe, (***b***) Al/3.1% Fe and (***c***) Al/4.7% Fe.

Reinforcement volume fraction, density, and porosity

The volume fraction of the wire reinforcement was calculated from the weight of the reinforcement preforms and the composite ingot. The weight fraction of the reinforcement was computed[16] using the recorded weights and converted to volume fraction by considering the density of aluminum to be 2.705 g/cm^3, the density of galvanized iron as 7.791 g/cm^3 and the presence of 10.8 volume percentage of zinc in the form of coating. The density of the monolithic aluminum alloy and the reinforced counterpart was measured using Archimedes' principle. Precise details of these measurements and calculations can be found elsewhere[14,15]. The densities, derived from the recorded weights, were compared with the theoretical value to help establish the volume fraction on micro-porosity.

Characterization of initial microstructure

Samples for microstructural characterization of the composite samples in the extruded condition were prepared using standard metallographic techniques. The polished and etched samples were examined in a Scanning Electron Microscope [SEM (Model JEOL JSM T330A)] equipped with energy dispersive spectroscopy (EDS). Examination of intrinsic microstructural features, both at low and high magnifications, helps determine: (i) the presence, nature and distribution of microscopic pores, and (ii) interfacial integrity between the reinforcing phase, i.e. galvanized iron wire, and the aluminum alloy metal matrix.

Coefficient of thermal expansion

CTE of both monolithic aluminum alloy and reinforced composite counterpart was determined using an automated vertical push rod-type thermo-mechanical analyser. The displacement experienced by samples of monolithic aluminum alloy and the composite was measured as a function of temperature in the range 50–400°C, using an alumina probe and in an atmosphere of argon. This value was used to determine the coefficient of thermal expansion. The heating rate of the samples was maintained at 10°C/min and gas, i.e. argon flow rate was maintained at 1.1 l/min. The experimentally determined value of CTE was correlated with the value predicted by classical theory. The equations used for comparing CTE are: (i) ROM (eq. (1)), and (ii) Schapery equation (eq. (2)) for longitudinal thermal expansion of continuous fibre-reinforced composites[17,18].

$$\alpha_C = \alpha_f V_f + \alpha_m V_m, \quad (1)$$

$$\alpha_C = [(\alpha_f V_f E_f + \alpha_m V_m E_m)/(V_f E_f + V_m E_m)]. \quad (2)$$

In eqs (1) and (2), α_c denotes the coefficient of thermal expansion of the composite material, and α_f V_f, E_f and

α_m, V_m, E_m denote the coefficient of thermal expansion, volume fraction and elastic modulus of the reinforcing fibre and the aluminum alloy metal matrix, respectively.

Mechanical properties

A systematic characterization of the mechanical properties of the composite samples was carried out using microhardness measurements and uniaxial tensile tests. Microhardness measurements were made on samples of the un-reinforced aluminum alloy and the reinforced counterpart using a digital microhardness tester. Microhardness measurements were made with a pyramidal diamond indenter having an included angle (i.e. face angle) of 136° using an indenting load of 25 gram-force for a dwell time of 15 s. For samples of the reinforced aluminum alloy metal matrix, microhardness measurements were made at the following locations: (i) the 1050 aluminum alloy matrix, (ii) the reinforcing galvanized wire, and (iii) at the matrix–reinforcement interfaces. Smooth bar tensile properties of both the monolithic alloy and the composite material were determined in accordance with procedures outlined in ASTM test method E8-96. The tensile tests were conducted on cylindrical specimens, having a gauge diameter of 5 mm and a gauge length of 25 mm, on a fully automated servo-hydraulic mechanical test machine [Model: INSTRON 8516] at an initial strain rate of 2.1×10^{-4}/s.

Analysis of fracture-failure

Fracture surface characterization studies were carried out on the deformed and failed samples of the monolithic aluminum alloy and the reinforced counterpart, so as to provide an insight into the macroscopic fracture mode and the intrinsic microscopic mechanisms governing fracture during uniaxial loading. The fracture surfaces were examined in an SEM equipped with EDS (Model: JEOL JSM-T330A).

Results

Density

Results pertaining to the volume fraction of the reinforcing phase, measurement of density and volume fraction (percentage) of micro-porosity are summarized in Table 1. The relatively lower volume fraction of porosity in the fibre-reinforced aluminum alloy metal matrix is an indication of the potential of the processing technique used, i.e. conventional casting followed by hot extrusion.

Initial microstructure

SEM observations of the wire reinforced aluminum alloy specimens revealed good interfacial integrity between the reinforcing wire and the aluminum alloy metal matrix (Figure 2). Evidence of limited interfacial reaction was distinctly observed at the fringes of the reinforcing wire (Figure 2).

Coefficient of thermal expansion

The results of CTE measurements on monolithic aluminum and its composite counterparts are shown in Table 2. The results reveal that the average value of the CTE of the 1050 aluminum alloy noticeably decreases with an incorporation of the reinforcing phase.

Table 1. Density and porosity for aluminum and its composites

Material	Density (g/cm^3)		Percentage porosity
	Theoretical	Experimental	
Monolithic Al	2.710	2.699 ± 0.0004	0.4 ± 0.2
Al/1.6% Fe	2.786	2.767 ± 0.006	0.7 ± 0.2
Al/3.1% Fe	2.862	2.834 ± 0.014	1.0 ± 0.5
Al/4.7% Fe	2.949	2.882 ± 0.020	2.3 ± 0.7

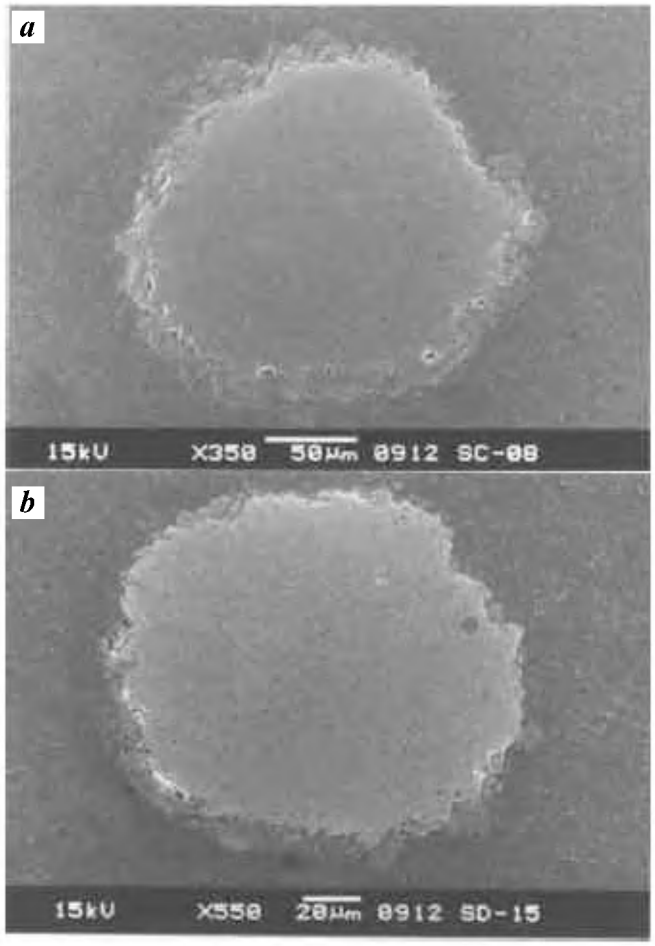

Figure 2. Representative SEM micrographs showing interfacial integrity between the reinforcement wire and the matrix in (***a***) Al/3.1% Fe, and (***b***) Al/4.7% Fe composites.

Hardness and tensile behaviour

The results of microhardness measurements made on the monolithic aluminum alloy and its composite counterpart are summarized in Table 3. The micro-hardness of the metal matrix containing 1.6% Fe and 3.1% Fe reinforcement was only marginally higher than that of the unreinforced aluminum alloy metal matrix. However, microhardness of the aluminum alloy containing 4.7% Fe ($H_v = 54$) was noticeably higher than that of the un-reinforced aluminum alloy metal matrix ($H_v = 43$). The hardness of the interfacial reaction zone was found to be noticeably higher than that of the reinforcing wire. Further, results reveal than an increase in volume fraction of the reinforcing phase causes a noticeable increase in the value of average microhardness of the metal matrix.

The results obtained from ambient temperature tensile tests are summarized in Table 4. Results reveal that the presence of wire preforms as the reinforcing phase causes a noticeable increase in elastic modulus, yield strength and ultimate tensile strength, with a concurrent degradation in ductility of the un-reinforced aluminum alloy metal matrix. The value of elastic modulus obtained by ROM was also computed in order to compare the experimentally determined value with the theoretical prediction. The upper and lower bounds of elastic modulus summarized in Table 4 were calculated as follows:

The upper bound value of elastic modulus using ROM was calculated by taking the elastic modulus of aluminum alloy AA1050 to be 68 GPa (average experimental value for aluminum alloy AA 1050) and that of galvanized iron wire reinforcement to be 200 GPa ($E = 200$ GPa)[19] and ignoring the presence of zinc, which has a lower elastic modulus ($E = 96.5$ GPa)[20].

The lower bound value of elastic modulus using ROM was calculated by assuming the elastic modulus of aluminum alloy 1050 to be 68 GPa (average experimental value for AA 1050) and galvanized iron to be 188.8 GPa. The elastic modulus of galvanized iron was computed by considering 0.108 volume fraction of zinc to be present as coating on the iron wire.

Table 2. Coefficient of thermal expansion of Al alloy AA1050 and its composites in the temperature range of 50–400°C

	Coefficient of thermal expansion (CTE) $\times 10^{-6}$		
Material	Exp. value	Schapery (7, 8)*	ROM*
Monolithic Al	26.6 ± 0.4	–	–
Al/1.6% Fe	26.3 ± 0.2	26.16	26.44
Al/3.1% Fe	25.3 ± 1.2	25.77	26.28
Al/4.7% Fe	24.9 ± 1.6	25.37	26.12

*Theoretical CTE values were corrected for the presence of Zn (CTE: 39.7×10^{-6}).

Table 3. Vickers microhardness (H_v) measurement

Material	Matrix	Wire	Interfacial zone
Monolithic Al	43 ± 1	–	–
Al/1.6% Fe	46 ± 1	166 ± 3	489 ± 60
Al/3.1% Fe	47 ± 1	158 ± 3	570 ± 44
Al/4.7% Fe	54 ± 2	175 ± 4	543 ± 20

Fracture behaviour

The tensile fracture surface features of the un-reinforced aluminum alloy and the composite counterpart are shown in

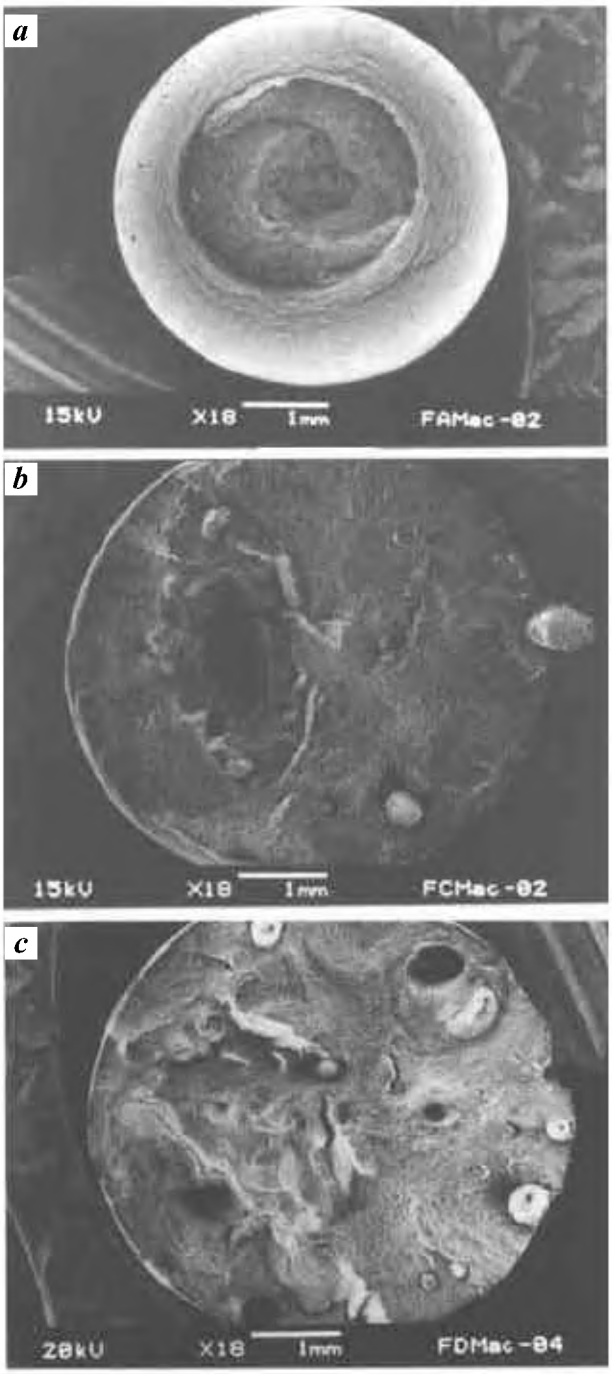

Figure 3. Representative low magnification SEM micrographs taken from tensile fracture surface of (*a*) monolithic aluminum, (*b*) Al/3.1% Fe and (*c*) Al/4.7% Fe composites.

Table 4. Room temperature tensile properties

Material	Elastic modulus (GPa)			0.2% YS (MPa)	UTS (MPa)	Ductility (%)
	Exp. value	ROM considering presence of zinc*	ROM ignoring presence of zinc**			
Monolithic Al	68 ± 2	–	–	117 ± 7	135 ± 12	24 ± 5
Al/1.6% Fe	74 ± 4	69.8	70.1	134 ± 11	155 ± 11	8 ± 1
Al/3.1% Fe	77 ± 1	71.7	72.0	165 ± 7	185 ± 6	3 ± 0.5
Al/4.7% Fe	80 ± 4	73.6	74.1	170 ± 35	195 ± 42	0.7 ± 0.2

*To get a lower bound, since Zn has lower elastic modulus (E_{Zn} = 96.5 GPa) when compared to iron.
**To get an upper bound, since Zn has lower elastic modulus when compared to iron (E_{Fe} = 200 GPa).

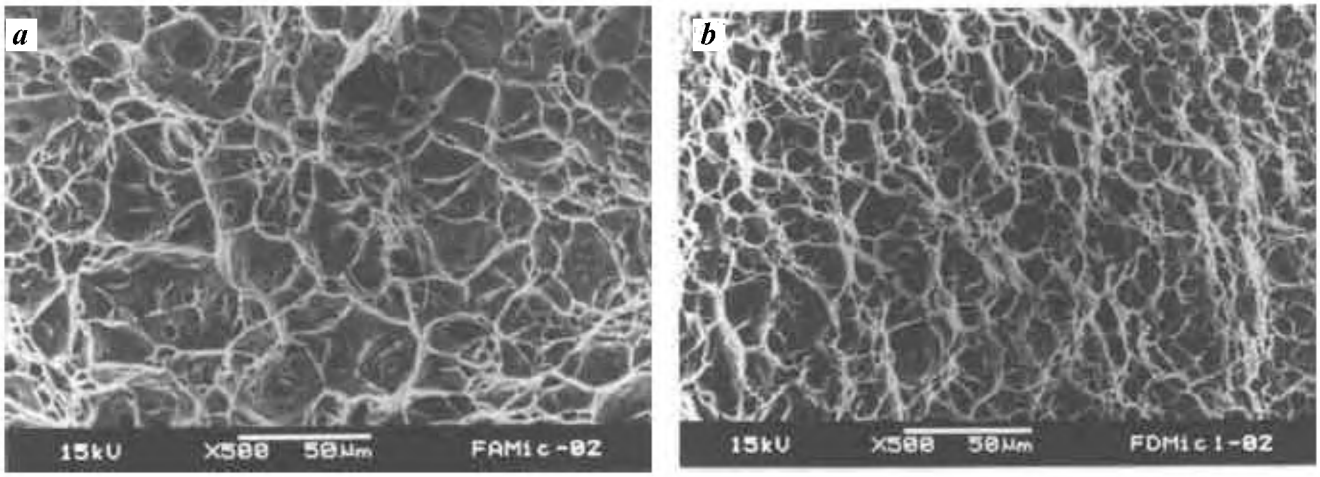

Figure 4. Representative SEM micrographs taken from tensile fracture surface of (***a***) monolithic aluminum and (***b***) Al/4.7% Fe composite showing matrix fracture characteristics.

Figures 3 and 4. SEM observations revealed a predominantly cup and cone type of fracture at the macroscopic level with dimples of varying size and shape at the microscopic level, indicative of localized micro plastic deformation. The composite material exhibited a mixed-mode fracture comprising transgranular and intergranular regions, with evidence of fibre breakage and fibre pull-out from the metal matrix. The matrix revealed: (i) a population of fine microscopic voids and dimples of varying sizes and shapes, indicative of locally ductile failure mechanisms and (ii) fibre pull-out and decohesion at matrix–fibre interfaces, indicative of locally brittle mechanisms.

Discussion

Synthesis of AAMMCs containing three different volume percentages of inter-connected wire preforms was successfully accomplished by conventional casting followed by hot extrusion. The effectiveness of this fabrication route to synthesize interconnected wire preform reinforced aluminum alloy metal matrix, even for low volume fraction of interconnected wire, i.e. 0.015, was evident from an absence of macroscopic pores and a minimal amount of fine microscopic pores in the material in the as-cast condition. The results of density and porosity measurements indicate that the fabrication methodology adopted is capable of minimizing porosity, thus enabling the production of near dense materials. Results of this study show the feasibility of the synthesis methodology to be a cost-effective alternative to several other cost-intensive methodologies currently in practice for fibre-reinforced MMCs[21–23].

Limited interfacial reaction was observed at the interface between the reinforcing wire and the aluminum alloy metal matrix (Figure 2). The interfacial integrity of the reinforcing iron wire with the aluminum alloy metal matrix is assessed in terms of interfacial debonding and presence of voids, and is found to be good for all of the composite samples examined in this study. The results reveal overall suitability of: (i) solidification processing parameters, such as melt superheat temperature, distance of deposition, and heat dissipation by mould material, and (ii) extrusion parameters to include soaking temperature, time, extrusion temperature and extrusion ratio, to govern the overall cooling rate and solidification of the matrix around the reinforcing phase.

Results of CTE measurement in the temperature range 50–400°C, revealed that the incorporation of interconnected wire reinforcement in the aluminum alloy metal matrix reduces the average CTE of the metal matrix. The

average experimental values of CTE for the Al/3.1%Fe and Al/4.7%Fe composites were lower than the theoretical predictions, and for Al/1.6% Fe, CTE was lower than the prediction made of ROM. The ROM is expected to give a higher value, since it generally assumes an upper limit. Even the Schapery equation, which uses a thermodynamic model to minimize the difference between the upper and lower bound solutions for long fibre reinforced metal matrices, predicted a marginally higher value than the experimental CTE for Al/3.1% Fe and Al/4.7% Fe composites. The lower value of longitudinal CTE exhibited by Al/3.1% Fe and Al/4.7% Fe composite specimens is attributed to the constraints induced by the reinforcing wire phase on preferential deformation and/or flow of the aluminum alloy metal matrix. This is consistent with the findings of other investigators who reported a decrease in CTE of the composite material with an increase in the reinforcing phase in the metal matrix[24,25]. For the Al/1.6% Fe composite, the observed marginal improvement in CTE is attributed to the lower-than-threshold volume fraction of the reinforcing phase that is capable of restraining expansion of the metal matrix. However, experimental CTE values overlap with those predicted by Schapery's model, if standard deviation is considered.

The results of microhardness measurements reveal the reinforced AAMMCs to exhibit significantly higher matrix hardness compared to the monolithic counterpart (Table 3). The average value of microhardness of the composite sample increases with an increase in volume fraction of the reinforcing phase in the aluminum alloy metal matrix. This can be attributed to the conjoint and mutually interactive influence of: (i) presence of a harder (158–175 H_v) reinforcing phase in the aluminum alloy matrix, and (ii) limited solid solution/age hardening of the metal matrix as a result of dissolution of zinc, which is present as a coating on the reinforcing wire.

The microhardness value of the matrix adjacent to the reinforcing wire, i.e. the interfacial zone, was found to be significantly higher than the un-reinforced metal matrix. The higher hardness exhibited by the interfacial region is ascribed to: (i) the formation and presence of intermetallic particles, and (ii) creation of pockets of high dislocation density in the aluminum alloy metal matrix adjacent to the reinforcing wire due to intrinsic differences in CTE between the matrix phase and the reinforcing wire phase.

Results of tensile tests revealed that the use of wire reinforcements in interconnected form causes an increase in elastic modulus (E), yield strength and ultimate tensile strength with a resultant degradation in ductility of the aluminum alloy matrix. The experimentally determined modulus values of the composite materials exceeded the value predicted by ROM (Table 4). The average elastic modulus of the composite material was significantly higher than the upper bound prediction using ROM. Considering standard deviation, the elastic modulus of the metal matrix containing 1.6 volume percentage of the wire reinforcement was well within the upper bound prediction of ROM. This is partially attributed to a lower volume fraction of the interconnected reinforcement. The resultant effectiveness of the interconnection of the reinforcing phase is not as significant as for the aluminum alloy metal matrix, which is reinforced with a higher volume fraction. A noticeable increase in elastic modulus of the MMC is attributed to the innate capability of the wire reinforcements, in inter-connected form, to effectively constrain deformation of the metal matrix when compared to the presence of individual iron wires or strands in the metal matrix. This is achieved by facilitating better load transfer within the wire network. The observed results are promising in developing an entirely new class of reinforced metal matrices for applications that demand high elastic modulus or stiffness as the primary criterion for design.

Results of tensile tests also reveal the composite materials to exhibit a higher offset (0.2%) yield strength and ultimate tensile strength when compared to the monolithic counterpart. The observed increase in strength of the composite microstructure is ascribed to good interfacial bonding between the reinforcing phase and the aluminum alloy metal matrix, which facilitates an efficient transfer of load from the metal matrix to the reinforcing fibres. The ultimate tensile strength of the composite material was noticeably higher than that of monolithic aluminum even after taking standard deviation into consideration, except for the metal matrix reinforced with 1.6 volume percentage of the wire reinforcement. The ductility of the composite material was inferior when compared to the un-reinforced aluminum alloy. The reduction in ductility of the composite material is attributed to a decrease in cavitation resistance of the aluminum alloy metal matrix. This reduction in cavitation resistance is due to: (i) the presence of a harder and stronger reinforcing phase, and (ii) the increased brittleness of the aluminum alloy as a consequence of dissolution of zinc from the reinforcing wire during processing, i.e. casting and extrusion. The results are consistent with the experimental findings documented in Tables 3 and 4 and shown in Figure 3.

Tensile fracture surface of the monolithic aluminum alloy showed the presence of a population of dimples, which is indicative of locally ductile failure mechanisms (Figures 3 and 4). The scanning electron micrographs of the composite samples revealed the following features: presence of pulled-out fibres, circular cavities, and isolated pockets of broken fibres. The presence of fibre pull-out suggests that during tensile loading, the initiation of crack and subsequent propagation is facilitated through the matrix–wire interfacial region. The presence of shallow cavities rather than deep circular cavities, further indicates the mutually interactive influence of: (i) failure of interconnections during tensile loading followed by fibre pull-out, and (ii) Partial damage of interconnections during extrusion and subsequent pull-out of the wire as a result of failure of the brittle interfacial zone during tensile loading.

The presence of a few broken fibres confirms that good interfacial bonding between the reinforcement (wire) and the metal matrix was realized during processing, enabling an effective load transfer between the reinforcing phase and the metal matrix. The matrix region of the composite revealed a predominantly mixed-mode fracture. Ductile fracture was evident in the matrix region, except at and near the wire reinforcements. The macroscopic difference in fracture surface features between the monolithic aluminum alloy samples (cup and cone; Figure 3 *a*) and the composite samples (relatively flat and featureless; Figures 3 *b* and *c*) indicates the increased brittleness of the aluminum alloy matrix as a result of the presence of wire-preform. This is well-supported by higher hardness exhibited by matrix of the aluminum alloy composite samples compared to the monolithic counterpart (Table 4).

In essence, results of CTE, hardness and tensile properties of the composite samples suggest that there is a threshold in the volume fraction of interconnected reinforcement that is required so as to affect an improvement in properties of the aluminum alloy matrix. The volume fraction is low for the case of interconnected reinforcements and is in the range between 1.6 and 3.1%. This observation concurs with the findings reported in an earlier study for the case of non-interconnected fibre-reinforced composites[26].

Conclusions

Based on the results of an investigation on the influence of reinforcement architecture and volume fraction on the mechanical response of 1050 aluminum alloy reinforced with galvanized wire, following are the key findings: (i) conventional casting technique followed by hot extrusion is an effective combination to synthesize interconnected galvanized iron wire reinforced metal matrix composites even for a low volume fraction of the reinforcement. (ii) An increase in volume fraction of the wire reinforcement leads to an increase in porosity levels, dimensional stability and hardness of the aluminum alloy matrix. (iii) The presence of interconnected wires in the form of preform increases the elastic modulus beyond the rule of mixture prediction for the case of Al/3.1% Fe and Al/4.7% Fe composites. The offset yield strength and the ultimate tensile strength of aluminum alloy AA1050 was enhanced by incorporating reinforcing wires in an interconnected form while the ductility was adversely affected.

1. Nair, S. V., Tien, J. K. and Bates, R. C., *Int. Met. Rev.*, 1985, **30**, 285–297.
2. Srivatsan, T. S. and Sudarshan, T. S. (eds), In *Rapid Solidification Technology: An Engineering Guide*, Technomic Publishing Inc, Lancaster, PA, 1993, pp. 603–700.
3. Taya, M. and Arsenault, R. J., In *Metal Matrix Composites: Thermomechanical Behavior*, Pergamon Press, Elmsford, New York, 1989, p. 4.
4. Allison, J. E. and Jones, J. W., Fatigue behaviour of discontinuously-reinforced metal-matrix composites. In *Fundamentals of Metal Matrix Composites* (eds Suresh, S., Mortensen, A. and Needleman, A.), Butterworth-Heinemann, London, 1993, pp. 269–296.
5. Hunt, Jr. W. H., Cost-effective high performance aluminum matrix composites for aerospace applications. In International Conference on PM Aerospace Materials, MPR Publishing, Laussane, Switzerland, 1991, pp. 32-1–32-15.
6. Hunt, Jr. W. H., Discontinuously-reinforced aluminum: The second generation. In *Processing and Fabrication of Advanced Materials III* (eds Ravi, V. A., Srivatsan, T. S. and Moore, J. J.), TMS: The Minerals, Metals and Materials Society, Warrendale, PA, 1994, pp. 663–690.
7. East, W. F., Metal-matrix composites take-off. *Mater. Eng.*, 1988, 33–36.
8. Suresh, S. and Chawla, K. K., In *Fundamentals of Metal Matrix Composites* (eds Suresh, S., Mortensen, A. and Needleman, A.), Butterworth-Heinemann, London, 1993, pp. 119–133.
9. Srivatsan, T. S., Sudarshan, T. S. and Lavernia, E. J., *Prog. Mater. Sci.*, 1995, **39**, 317–409.
10. Lewandowski, J. J., In *Metal Matrix Composites* (ed. Clyne, T. W.), Elsevier Publishers, 2000, vol. 3, pp. 151–187.
11. Clyne, T. W. and Withers, P. J., In *An Introduction to Metal Matrix Composites*, Cambridge University Press, UK, 1993, p. 122.
12. Lloyd, D. J., *Int. Mater. Rev.*, 1994, **39**, 1–23.
13. Ganesh, V. V. and Gupta, M., *Mater. Sci. Technol.*, 2001, **17**, 1465–1471.
14. Ganesh, V. V., *Mater. Sci. Eng.*, 2002, **333**, 193–198.
15. Srikanth, N., Ganesh, V. V. and Gupta, M., *Mater. Sci. Technol.*, 2003, **19**, 48–54.
16. Davis, J. R., Lee, C. K. and Gupta, M. and Associates, *ASM Specialty Handbook, Aluminum and Aluminum Alloys*, ASM International Publications, Materials Park, OH, USA, 1993.
17. Vaidya, R. U. and Chawla, K. K., *Composites Sci. Technol.*, 1994, **50**, 13–22.
18. Asthana, R., *Adv. Perform. Mater.*, 1998, **5**, 213–255.
19. Bauccio, M. (ed.), In *Metals Reference Book*, ASM International Publication, OH, USA, 1993, 3rd edn, p. 311.
20. Ross, R. B., In *Metallic Materials Specification Handbook*, E.&F. N. Spon Ltd, London, UK, 1972, p. 701.
21. Everett, R. K. and Arsenault, R. J., In *Metal Matrix Composites: Processing and Interface*, Academic Press, New York, 1991, pp. 64–67.
22. Seshan, S., Guruprasad, A., Prabha, M. and Sudhakar, A., *J. Indian Inst. Sci.*, 1996, **76**, 1–14.
23. Vassel, A., *Mater. Sci. Eng. A*, 1999, **263**, 305–313.
24. Ganesh, V. V. and Gupta, M., *Scr. Mater.*, 2001, **44**, 305–310.
25. Tao, L. and Delannay, F., *Acta Mater.*, 1998, **46**, 6497–6509.
26. Friend, C. M., *J. Mater. Sci.*, 1987, **22**, 3005.

ACKNOWLEDGEMENTS. We thank the anonymous reviewer for comments, corrections and suggestions to improve the manuscript.

Received 23 August 2004; revised accepted 17 November 2004